Zoosyst. Evol. 101 (3) 2025, 1197–1211 | DOI 10.3897/zse.101.155510

PENSOFT

für Naturkunde MUSEUM FÜR NATURKUNDE BERLIN

Molecular phylogeny and taxonomy of the *Sicista concolor* group (Mammalia, Rodentia, Sicistidae) with the description of a new species

Yu Deng[1*], Qing Liu[1*], Xuming Wang[2], Binbin V. Li[3,4], Jing Wang[1], Shuang Liu[1], Rui Liao[2], Shaoying Liu[2], Shunde Chen[1]

1 *College of Life Science, Sichuan Normal University, Chengdu 610101, China*
2 *Sichuan Academy of Forestry, Chengdu 610081, China*
3 *Environmental Research Center, Duke Kunshan University, Kunshan, Jiangsu 215316, China*
4 *Nicholas School of the Environment, Duke University, Box 90328, Durham, NC 27708, USA*

https://zoobank.org/A0E0716F-3E4F-442E-B7C8-C3C78C9A41B7

Corresponding authors: Shaoying Liu (shaoyliu@163.com); Shunde Chen (csd111@126.com)

Academic editor: Melissa T. R. Hawkins ♦ **Received** 11 April 2025 ♦ **Accepted** 30 May 2025 ♦ **Published** 14 July 2025

Abstract

Sicista is the sole extant genus in the family Sicistidae and one of the most ancient rodent genera known to date. This genus is of particular importance in mammalian evolutionary studies due to its ancient lineage and specialized ecological niches. In China, species of the genus *Sicista* are notoriously rare and elusive, making specimen collection exceptionally difficult. *Sicista concolor* is a poorly studied species within the genus, and its phylogenetic relationships and evolutionary history remain largely unexplored. In this study, we collected 36 specimens of *S. concolor*, sequenced one mitochondrial gene and two nuclear genes, and conducted morphological analyses, with particular emphasis on penile morphology, to infer its phylogenetic relationships. Our findings reveal that *S. concolor* represents a species complex comprising four distinct species. We describe a new species, *Sicista meiguites* **sp. nov.**, and elevate the subspecies *S. c. weigoldi* to full species status. Our molecular analyses also revealed a cryptic species.

Key Words

New species, *Sicista concolor* group, taxonomy

Introduction

The mountainous region of southwest China has garnered significant attention for its remarkable species diversity. In recent years, the discovery of new species in this region has shown a consistent upward trend (Wilson and Reeder 2005; Jiang et al. 2015), particularly among small mammals (Chen et al. 2017; Liu et al. 2019; Pu et al. 2022). This implies that species richness in southwest China is significantly underestimated, especially for some original taxonomic groups that need to be re-evaluated (Chen et al. 2017; Zhao et al. 2023; Yang et al. 2025).

Dipodoidea is a superfamily within the suborder Myomorpha of the order Rodentia. *Sicista* is one of the most enigmatic genera in this superfamily and represents the only extant genus of the family Sicistidae (Lebedev et al. 2013; Pisano et al. 2015). Compared to the highly specialized, obligate bipedal jerboas (Dipodidae) and the facultatively bipedal jumping mice (Zapodidae), birch mice are relatively unspecialized in their locomotor adaptations (Lebedev et al. 2019). The genus currently comprises 14 to 17 species, which are distributed across the Palearctic region (Lebedev et al. 2019). These species are distributed in temperate lowland and montane forests, steppes, as

* These authors contributed equally to this work.

well as subalpine shrublands and meadows (Holden and Musser 2005; Baskevich 2016; Holden et al. 2017).

The morphological characteristics of species within the genus *Sicista* are relatively conserved, making it challenging to distinguish between them based solely on external features. Moreover, wild populations are scarce, and specimens are exceedingly rare, which further complicates taxonomic studies. To this day, the taxonomic issues within the genus remain unresolved. At least four species of *Sicista* are currently recognized in China: *Sicista subtilis* (Pallas 1773), *Sicista concolor* (Büchner 1892), *Sicista tianschanica* (Salensky 1903), and *Sicista caudata* (Thomas 1907) (Jiang et al. 2015). Cserkész et al. (2017) suggested that *Sicista pseudonapaea* (Strautman 1949) is also distributed in China. *S. pseudonapaea* was also accepted in Wei et al. (2024). Lebedev et al. (2019) divided the genus *Sicista* into five major clades, among which are *tianschanica*, *concolor*, *caudata*, *betulina*, and *caucasica*. The *concolor* lineage (*S. concolor* group), which includes *S. concolor*, *Sicista weigoldi* (Jacobi 1923), and *Sicista leathemi* (Thomas 1893), is one of the most enigmatic and elusive groups. *S. concolor* was first documented by Büchner in 1892 in Xining, Qinghai Province (formerly Xining, Gansu Province) and is primarily distributed in the northeastern region of the Qinghai-Tibet Plateau. The relatively obscure *Sicista leathemi* was typically considered a subspecies of *S. concolor* (Lebedev et al. 2019; Wei et al. 2024). Meanwhile, *Sicista weigoldi* was found in the western parts of Sichuan and Yunnan Provinces (Holden et al. 2017). The birch mouse has a notably long hibernation period during the winter and a brief breeding season in summer, coupled with relatively low reproductive rates (Holden et al. 2017). As a result, its wild population density remains sparse, and specimens are exceedingly rare (Cheng et al. 2021). As of now, the relationships among the *S. concolor* group continue to be a matter of debate (Lebedev et al. 2019).

In this study, we conducted intensive sampling across the southwestern mountains and their surrounding areas, ultimately collecting 36 specimens of the *S. concolor* group. We examined the Chinese birch mouse populations from different regions and investigated the phylogeny and evolutionary relationships between these groups. Our findings offer new insights into the phylogenetic relationships and evolutionary history of *Sicista*, providing valuable reference material for future taxonomic studies.

Materials and methods

Molecular data and analyses

A total of 36 specimens of the *S. concolor* group were collected from Sichuan and Qinghai provinces in China (Fig. 1, Suppl. material 1). Each specimen was assigned a unique identification number, and various external measurements were recorded, including head-body length (HBL), tail length (TL), ear length (EL), and hind foot length (HFL). Fresh liver or muscle tissue was collected from each specimen and preserved in 99% pure analytical ethanol. Upon returning to the laboratory, tissue samples were transferred to -80 °C for molecular analysis after replacing the ethanol. The specimens and tissue samples used in this study were stored at the Sichuan Academy of Forestry (SAF) and the College of Life Sciences, Sichuan Normal University (SCNU), respectively. All animal experiments for this project were approved by the Ethics Committee of Sichuan Normal University. No human subjects were used in this study.

Total DNA was extracted using a rapid DNA extraction kit for animal tissue (Chengdu Fuji Biotechnology Co. Ltd.). The PCR protocol included 35 cycles, starting with an initial denaturation step at 94 °C for 5 minutes, followed by denaturation at 94 °C for 45 seconds, annealing at 49–60 °C for 45 seconds, extension at 72 °C for 90 seconds, and a final extension at 72 °C for 10 minutes. We amplified one mitochondrial gene, cytochrome *b* (CYTB, 1140 bp), and two nuclear genes: a partial fragment of the inverted repeat-binding protein (IRBP, 711 bp) and the growth hormone receptor (GHR, 528 bp). Specific primers described by Lebedev et al. (2013, 2019) were used for PCR amplification. These markers are well-established for assessing phylogenetic relationships in mammals (Meredith et al. 2011; He et al. 2017). Sequencing was carried out by Beijing Qingke Biotechnology Co., Ltd. The resulting sequences were aligned using MEGA v.5.0 software (Tamura et al. 2011) and verified to ensure correct reading frames and the absence of stop codons. Outgroup sequences were downloaded from GenBank (Suppl. material 1).

The following three datasets were employed in the analysis: (I) the mitochondrial dataset (CYTB), (II) the nuclear gene dataset (nuDNA), and (III) the combined mitochondrial and nuclear gene dataset (mtDNA + nuDNA). To determine the optimal model for phylogenetic analysis, we utilized jModelTest v.2.1.7 (Darriba et al. 2012). The best-fit models for each gene, selected using the Akaike Information Criterion (AIC) (Luo et al. 2010).

Tree reconstruction was performed using both maximum likelihood (ML) and Bayesian inference (BI) methods. The Bayesian tree was constructed using BEAST v.1.7.5 (Drummond et al. 2012), and the posterior probabilities (PP) for each node were calculated. The XML input file was prepared in BEAUti v.1.7.5, with model settings based on the best-fit substitution models for each gene as determined by AIC. The system tree was generated with 100,000,000 MCMC generations, with samples taken every 5000 generations. The relaxed uncorrelated exponential clock model and the Yule speciation model were applied during the analysis. Default prior values for all other parameters were used (Liu et al. 2017). Convergence of the MCMC chains was assessed using Tracer v.1.6 (Rambaut and Drummond 2013) by examining the log files. Results were considered stable and reliable when the effective sample sizes (ESSs) exceeded 200. The burn-in phase was conducted in TreeAnnotator v1.6 (Rambaut 2016) to discard the initial samples, and the maximum clade credibility tree was generated. ML analysis was performed using RAxML v.7.2.8 (Stamatakis et al. 2008) on the CIPRES Science Gateway v3.1 (Miller et al. 2010).

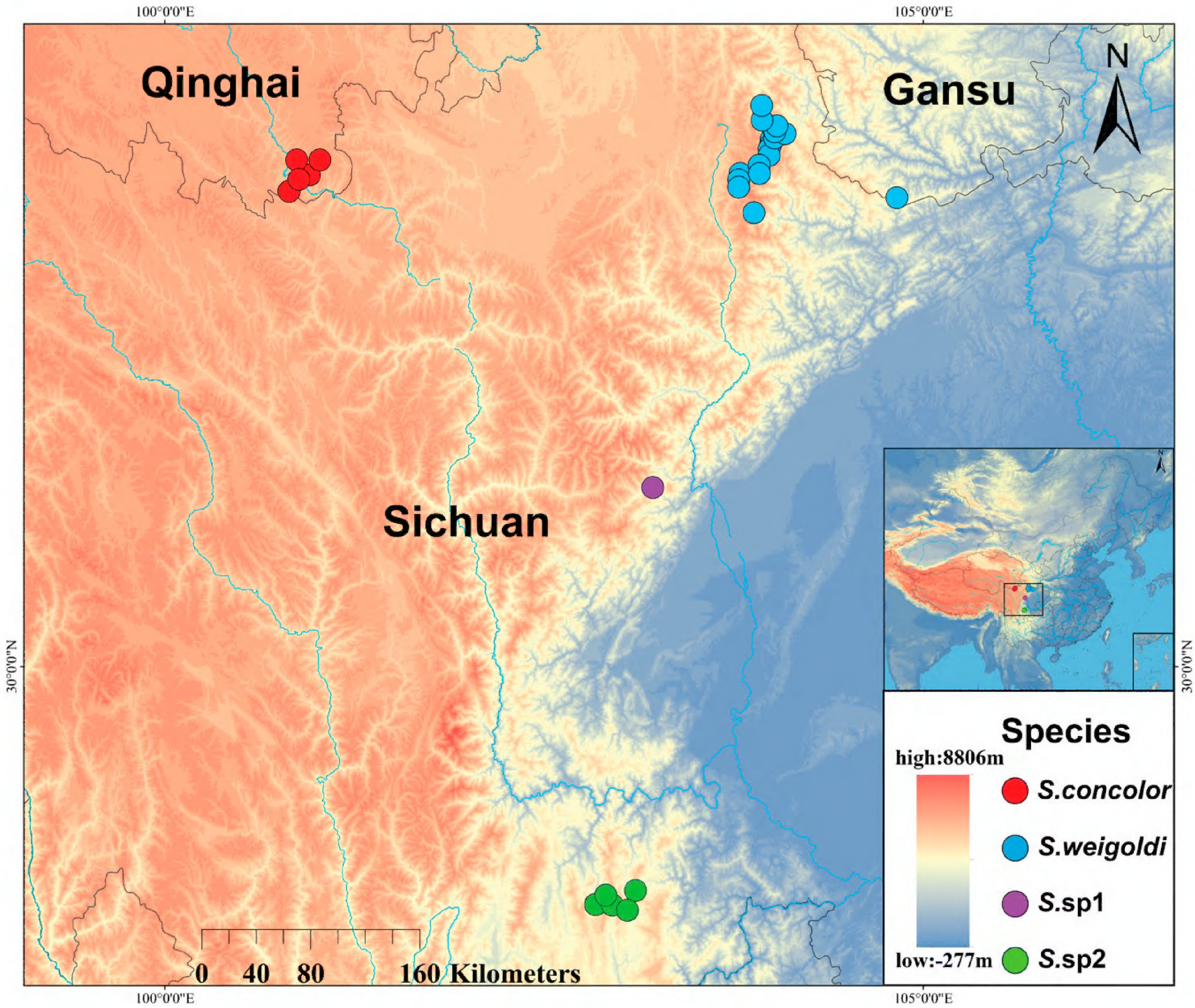

Figure 1. Map of the collection sites of the *S. concolor* group in this study.

Nodes with bootstrap support (BS > 70) were considered to have significant support in the ML tree. Genetic distances were calculated based on the CYTB gene using the Kimura two-parameter (K2P) model (Kimura 1980) in MEGA v.5.0 (Tamura et al. 2011), with 1000 bootstrap replicates.

Phylogenetic analysis reveals significant genetic differences between populations, leading to the use of two separate datasets: nuDNA (ii) and mtDNA + nuDNA (iii). Species trees generated from these datasets serve as the primary phylogenetic trees. The hypothesis of independent evolutionary lineages represented by these populations was tested using BPP v3.1 (Yang and Rannala 2010). In BPP, 12 parameter combinations were tested, with the results clearly distinguishing species differentiation. Time-calibrated mitochondrial gene trees were employed for GMYC analysis (Pons et al. 2006), with outgroups removed, and species identification was conducted using the split package in R (Paradis et al. 2004).

Divergence times based on the nuDNA dataset were estimated in BEAST v1.7 (Drummond et al. 2012). All fossil calibration age constraints were treated as lognormal distributions (Ho 2007). To estimate divergence times, we used two fossil calibration points following the approaches of Wu et al. (2012) and Lebedev et al. (2019). The first calibration was based on the estimated origin of Murinae, constrained between 7.30 and 12.90 Ma (mean = 9.50, standard deviation = 0.177), which serves to calibrate the deeper split between Dipodidae and Muridae. The second calibration point corresponds to the divergence between *Sicista subtilis* and *S. betulina*, set at approximately 2.60 Ma (mean = 2.6, standard deviation = 0.1), consistent with the early fossil record of the genus *Sicista* (Kowalski 2001).

Morphological data and analyses

The skull measurements were taken using a digital vernier caliper with an accuracy of 0.01 mm, while external morphological data were obtained from field measurements accurate to 1 mm (Yang et al. 2005). Body weight (BW), head-body length (HBL), tail length (TL), hind foot length (HFL), ear length (EL), palatal length (PL), skull basal length (SBL), median palatal length (MPL), zygomatic breadth (ZB), least breadth between the orbits (LBO), braincase breadth (BB), braincase height (BH), auditory bulla length (ABL), upper toothrow length (UTRL), length of upper molars (LUM), upper molar row breadth (UMRB), mandibular length (ML), lower toothrow length

(LTRL), and length of lower molar row (LLMR). Adult specimens were distinguished from juveniles and subadults based on the degree of molar tooth wear, which is a commonly used and reliable criterion in small mammal taxonomy and age classification (Lu et al. 1987).

Based on the skull measurement indices mentioned above, SPSS v17.0 was used for analysis. When the data meet the normal distribution, principal component analysis (PCA) was used to evaluate the overall similarity among various groups of individuals, and discriminant function analysis (DFA) was used to determine whether the classification was correct.

In addition, we recorded the morphological characteristics of the male glans penis (Hooper 1958). We prepared the glans penis using standard methods (Hooper 1958; Lidicker 1968) and depicted the bacula structure (Yang and Fang 1988). The glans were stored in 75% ethanol for 1–19 years. The anatomy was performed under a binocular microscope to observe and describe the morphology of the urethral opening, dorsal papilla, and outer crater papilla. The bacula were preprocessed by appropriate methods (Liu et al. 2007, 2012).

Results

Molecular results

Using three datasets, we reconstructed the phylogenetic relationships of the *S. concolor* group employing both ML and BI methods, and the resulting topologies were largely consistent (Fig. 2). These phylogenetic trees strongly support the hypothesis that the *S. concolor* group comprises at least four distinct clades (PP > 0.9, BS > 70). *S. concolor* is from Qinghai Province. *S.* sp2 from Megu, Sichuan Province, is sister to *S.* sp1. *S. weigoldi* from the Songpan region and its surroundings forms a sister group to both *S.* sp1 and *S.* sp2. These results provide valuable phylogenetic evidence for the internal classification of the *S. concolor* group.

The average genetic distances between the four branches of the *S. concolor* group based on the CYTB gene are shown in Table 1. The results indicate that the genetic distance between *S.* sp1 and *S. concolor* is 0.179, followed by 0.156 between *S.* sp1 and *S. weigoldi*. The genetic distances between *S.* sp2 and *S. concolor* and *S. weigoldi* are 0.185 and 0.166, respectively. The smallest genetic distance, 0.139, is observed between *S.* sp1 and *S.* sp2. These genetic distances highlight clear interspecific differentiation.

Table 1. Kimura two-parameter (K2P) genetic distances in the *S. concolor* group based on the CYTB gene.

Average genetic distance (%)	*S.* sp1	*S.* sp2	*S. concolor*
S. sp1			
S. sp2	0.139		
S. concolor	0.179	0.185	
S. weigoldi	0.156	0.166	0.181

Results from the GMYC analysis support the delimitation of the four clades as four distinct species (Suppl. material 2). *S.* sp1 was excluded due to having one sample, which prevents reliable estimation of population parameters and may lead to unstable results (Yang and Rannala 2010; Yang 2015). The BPP results yielded posterior probabilities exceeding 0.95, strongly supporting the recognition of three valid species: *S. concolor*, *S. weigoldi*, and *S.* sp2 (Suppl. material 3).

The phylogenetic relationships depicted by the time-calibrated tree largely mirror those of the mitochondrial DNA (mtDNA) gene tree (Fig. 3). The topology of the time tree clearly indicates that the *S. concolor* group is subdivided into four distinct clades. Divergence time estimates suggest that the split between *S. tianschanica* and its sister clades dated to the Miocene, approximately 8.96 million years ago (95% credible interval [CI]: 4.26–17.21 Ma). The *S. concolor* group is divided into four primary clades, with its initial divergence occurring around 5.87 Ma (95% CI: 2.40–12.17 Ma). The most recent common ancestor of the three clades—*S.* sp1, *S.* sp2, and *S. weigoldi*—was estimated at 4.73 Ma (95% CI: 1.82–9.97 Ma). Finally, the divergence between *S.* sp1 and *S.* sp2 occurred at 2.96 Ma (95% CI: 0.78–6.79 Ma). Overall, the major differentiation events within the *S. concolor* group took place primarily between 2.96 and 5.87 Ma (Fig. 3).

Morphological results

A total of 14 skull measurements and four contour characteristics were recorded for the three putative species (excluding the skull of *S.* sp1). Due to severe damage to the skull of *S.* sp1, complete measurements could not be obtained, and thus it was excluded from the morphological analysis. As the shape index is highly susceptible to variation under field conditions, it was not considered reliable for morphological analysis. Among the skull indicators, ZB was excluded from the analysis because many specimens had damaged cheekbones during preparation, leaving only 13 variables for morphological analysis. Based on population type and skull size, juveniles and subadults were first removed, ensuring that only adult specimens were included in the analysis.

The Kaiser-Meyer-Olkin (KMO) measure of sampling adequacy was 0.781, and Bartlett's test showed statistical significance ($p < 0.001$), confirming that the data were suitable for PCA. For the *S. concolor* group, two principal components were selected, explaining a total of 76.15% of the variation. Among them, the first principal component (PC1) accounted for the largest proportion, at 64.48%. The factor loadings for PC1 were all positive, with UTRL, SB, MPL, UMRB, LTRL, BB, LLMR, and ML exceeding 0.8, indicating that these variables contributed the most to PC1 (Table 3). The second principal component (PC2) explained 11.66% of the variation, with mostly negative factor loadings, except for LUM, which had a loading greater than 0.5, suggesting its relevance to PC2 (Table 3). A scatter plot (Fig. 4a) shows

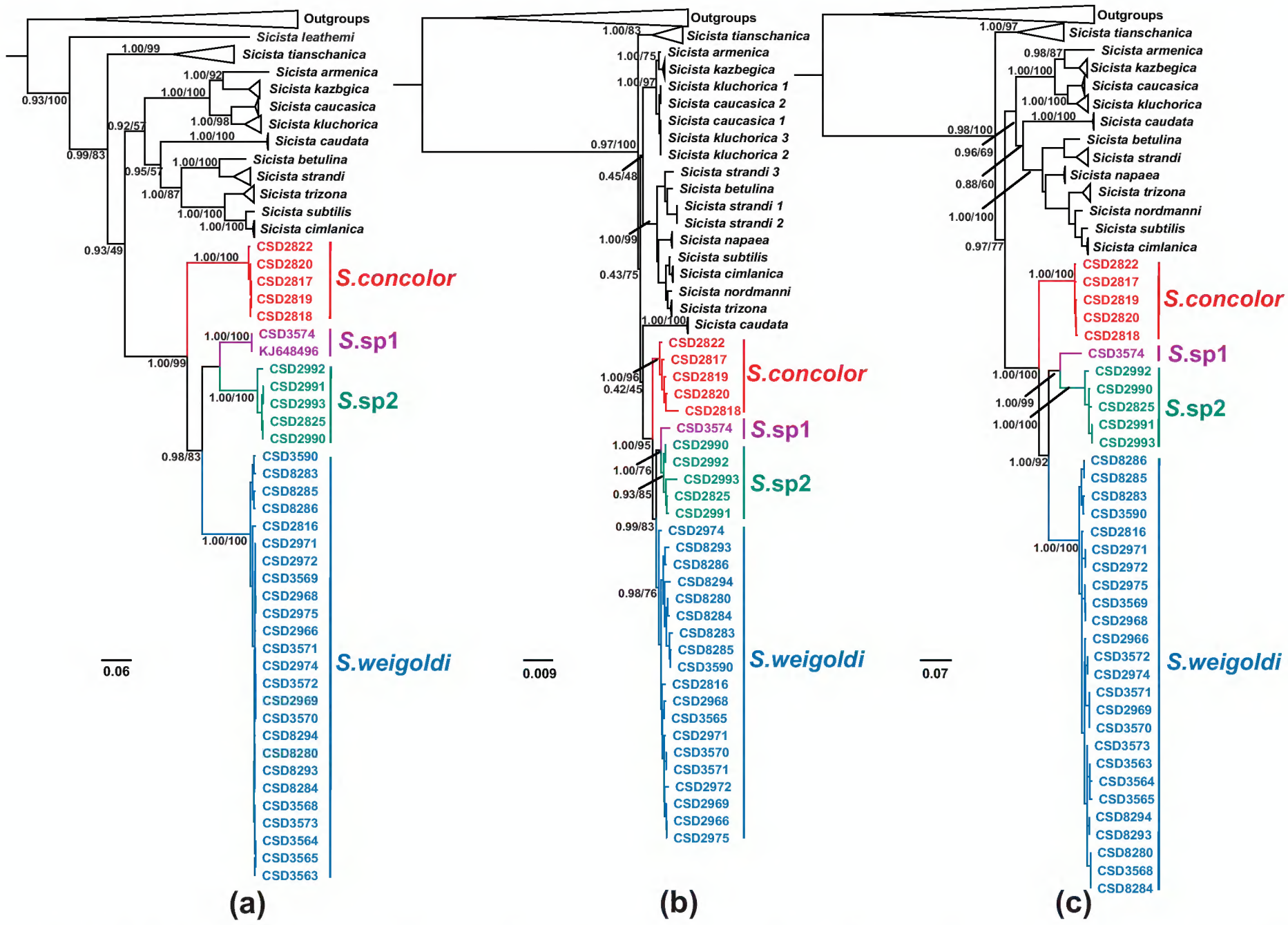

Figure 2. Bayesian and ML phylogenetic analyses based on the three datasets. **a.** dataset I (CYTB); **b** dataset II (IRBP+GHR, nuDNA), and **c.** dataset III (CYTB+IRBP+GHR, mtDNA+nuDNA). Numbers above or below branches correspond to Bayesian posterior probabilities and ML bootstrap values.

that while individuals of different species exhibit some overlap, a clear clustering pattern can still be observed.

Discriminant analysis of the three proposed species in this group (Fig. 4b) clearly distinguished between clades A, B, and C. The analysis showed that 100% of the original group samples were correctly classified, while cross-validation confirmed that 79.3% of the samples were correctly classified.

We compared the penile morphology of *S. concolor*, *S. weigoldi*, and *S.* sp2 within the *S. concolor* group and found significant differences among them (Fig. 5, Table 4). The glans penis of *S.* sp2 is elongated, with a Y-shaped urethral opening, and the baculum exhibits an ossified, rod-like structure (Fig. 5b1–b4). In contrast, both *S. concolor* and *S. weigoldi* have a short and thick glans penis, with a similar baculum morphology featuring two lateral wings at the tip (Fig. 5a, b). However, *S. weigoldi* differs in that its urethral opening is not Y-shaped (Fig. 5c1).

Discussion

The Chinese birch mouse (*S. concolor*) was first described by Büchner in 1892. Thomas (1912) collected two female specimens from Lintan, Gansu Province. Howell (1929) subsequently collected a subadult specimen from Yimianpo, in the former Manchuria. In 1940, Allen questioned the eastern extension of the distribution of *S. concolor* and suggested that *S. weigoldi* might be a junior synonym of *S. concolor*. Ellerman and Morrison-Scott (1951) recognized four subspecies within *S. concolor*: *S. c. concolor*, *S. c. flavus*, *S. c. leathemi*, and *S. c. tianschanica*. Later, *S. c. flavus* was described from the geographical range inhabited by *S. c. leathemi*, but since it was only known from the type specimen. It was considered a junior synonym of *S. c. leathemi* (Holden et al. 2017). Corbet (1978) expanded the subspecies of *S. concolor* to include *S. c. concolor*, *S. c. caucasica*, *S. c. caudata*, *S. c. leathemi*, and *S. c. tianschanica*. Wilson and Reeder (1993) maintained the placement of the genus *Sicista* within the Zapodidae family, recognizing *S. c. flavus*, *S. c. leathemi*, and *S. c. weigoldi* as subspecies. Smith et al. (2008) affirmed *S. concolor* as a distinct species but did not discuss the differentiation of subspecies. Cserkész et al. (2017) suggested that *S. concolor* might be a basal species within the genus *Sicista*. Additionally, *S. concolor* and *S. weigoldi*, which is typically regarded as a subspecies of the former, exhibit significant genetic divergence, with mitochondrial DNA studies indicating a genetic distance of more than 11% (Lebedev et al. 2019).

Our study incorporated many *S. concolor* specimens and provided a comprehensive review and revision of its

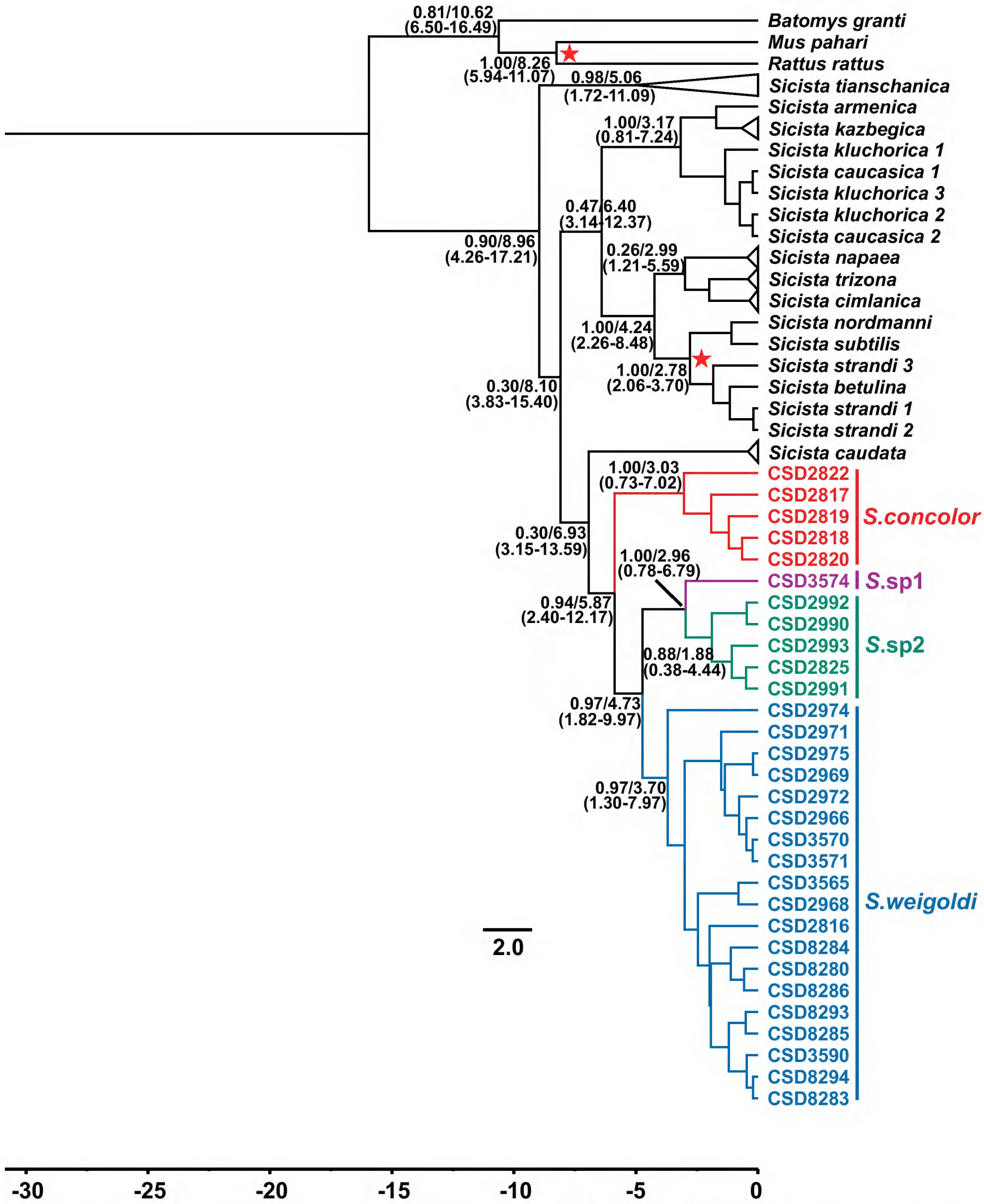

Figure 3. Divergence times were estimated using BEAST based on the nuDNA dataset. Branch lengths represent time. Numbers to the left of the dash indicate posterior probabilities (PP), while numbers to the right represent the median divergence time. Numbers within parentheses denote the confidence interval. The two red asterisks mark fossil-calibrated nodes.

phylogenetic relationships within the genus *Sicista*, as well as its taxonomic status. Through morphological differentiation, particularly the examination of penile characteristics, and the integration of molecular data, we reassessed the taxonomy of *S. concolor*. The results indicate that the species diversity of *S. concolor* has been underestimated, with at least three distinct species within the group. *S. concolor* is distinguished from *S. subtilis* by its unicolored dorsal fur and the absence of distinct black stripes. Specimens from Qinghai Province (*S. concolor*) exhibit pelage and skull characteristics that are largely consistent with the original description. Phylogenetic trees indicate that *S. concolor*

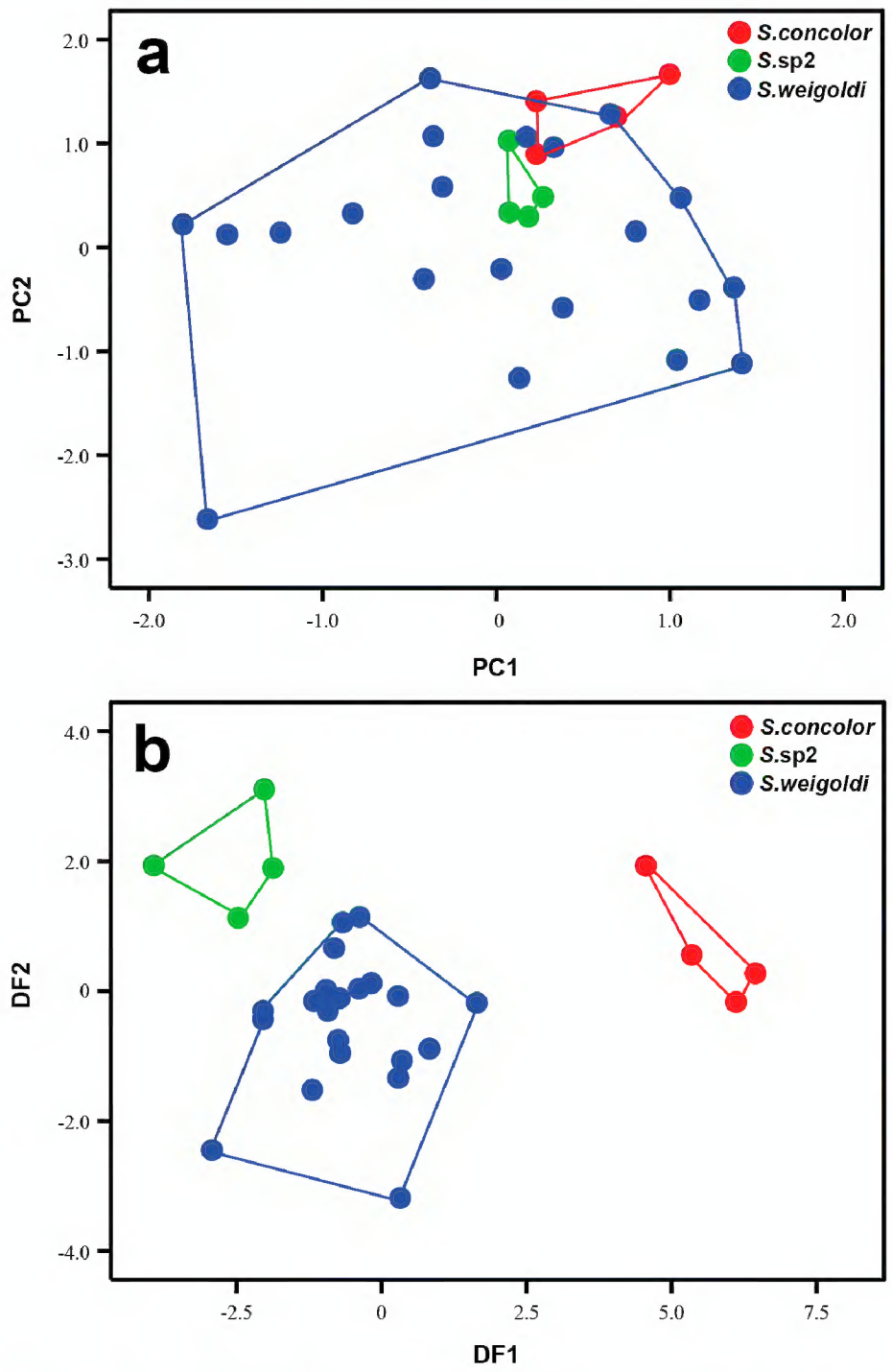

Figure 4. Results of the PCA (**a**) and the discriminant analysis (**b**) of 13 craniodental measurements of the *S. concolor* group.

forms a distinct clade, genetically separated from other regional groups, with a genetic distance greater than 11% (Table 1). The species delimitation results (Suppl. materials 2, 3) also support *S. concolor* as a valid species.

S. weigoldi (Jacobi 1923) was originally described from Songpan, characterized by its bicolored tail with a small brown patch at the tip, contrasting with the white underside, and the molar cusps with nearly no wear. The original description noted that the tail length was approximately 125% of the body length. However, based on specimens we collected from Songpan and surrounding areas, the tail length is found to be about 160–200% of the body length. Since the original record was based on a single specimen, we question the tail-to-body length ratio in the type specimen of *S. weigoldi*. Aside from this, other characteristics remain consistent with the original description (Fig. 7b1–b3). Additionally, the type specimen was captured in shrubland at an elevation of 3300–3750 meters in Songpan County, and our samples from Songpan were also collected at an elevation of 2980–3650 meters. Therefore, the clade from Songpan and surrounding areas is identified as *S. weigoldi*. Phylogenetic analysis of nuclear and mitochondrial genes reveals clear genetic divergence between *S. weigoldi* and other clades (Fig. 2, Table 1). Based on both morphological and molecular evidence, *S. weigoldi* is now recognized as a valid, independent species.

Based on both morphological and molecular differences (Fig. 2, Table 4), *S.* sp2 is described as a new species within the genus *Sicista*, named *Sicista meiguites* sp. nov. after its collection site in Meigu. This species is distinguished by its unique tail (Fig. 7b1–b3). The tail is darker than that of other species, displaying a deep brown color with a tuft of black hairs at the tip, and its length is approximately twice the length of the body. The palatine foramen in the upper jaw is positioned along a line connecting the protocone and paracone of the second molar, and its distance exceeds the width of the incisor foramen. The phylogenetic analysis, species delimitation using GMYC and BPP, principal component analysis, and discriminant function analysis all consistently support *S.* sp2 as a valid new species.

Specimens from Wenchuan (*S.* sp1) and Jiajin Mountain form a clade that is sister to the Meigu clade. We excluded *S.* sp1 from the PCA and BPP analyses due to severe damage to the skull and pelage. All our results strongly support the hypothesis of three distinct species (*S. concolor*, *S. weigoldi*, and *S. meiguites* sp. nov.). Although *S.* sp1 is strongly supported as a distinct lineage based on molecular data, the limited number of specimens, absence of male glans penis, and incomplete cranial morphology prevent a formal taxonomic diagnosis. We therefore tentatively treat it as a cryptic species, with its taxonomic status requiring further morphological and genetic evidence for confirmation.

According to the original description, *Sicista leathemi* (Thomas 1893) exhibits distinct differences compared to other *Sicista* species. The tail is distinctly bicolored, with brown on the upper side and white on the underside. The incisor foramina are shorter, extending posteriorly only to the middle level of the first molar. Liu et al. (2025) reported the presence of *S. leathemi* (GenBank: PQ227707) in Tibet, China, with both mitochondrial gene sequences and morphological evidence supporting its recognition as a valid species. Due to geographical isolation caused by mountain ranges and rivers and the considerable genetic distance from other groups, *S. leathemi* is currently considered a valid species.

Divergence time estimates suggest that *Sicista tianschanica* diverged from its sister lineages during the Miocene, approximately 8.96 Ma (95% CI: 4.26–17.21 Ma). Within the *S. concolor* group, the earliest divergence occurred around 5.87 Ma (95% CI: 2.40–12.17 Ma), resulting in the formation of four major clades. The most recent common ancestor of *S.* sp1, *S.* sp2, and *S. weigoldi* was dated to 4.73 Ma (95% CI: 1.82–9.97 Ma), followed by the divergence between *S.* sp1 and *S.* sp2 at approximately 2.96 Ma (95% CI: 0.78–6.79 Ma). Overall, the primary diversification events within the *S. concolor* group occurred between 5.87 and 2.96 Ma, spanning the Late Miocene to Late Pliocene. This timeframe aligns closely with major tectonic episodes associated with the uplift of the eastern and southeastern margins of the Qinghai-Tibet Plateau (QTP). Geological evidence indicates that the QTP experienced accelerated uplift

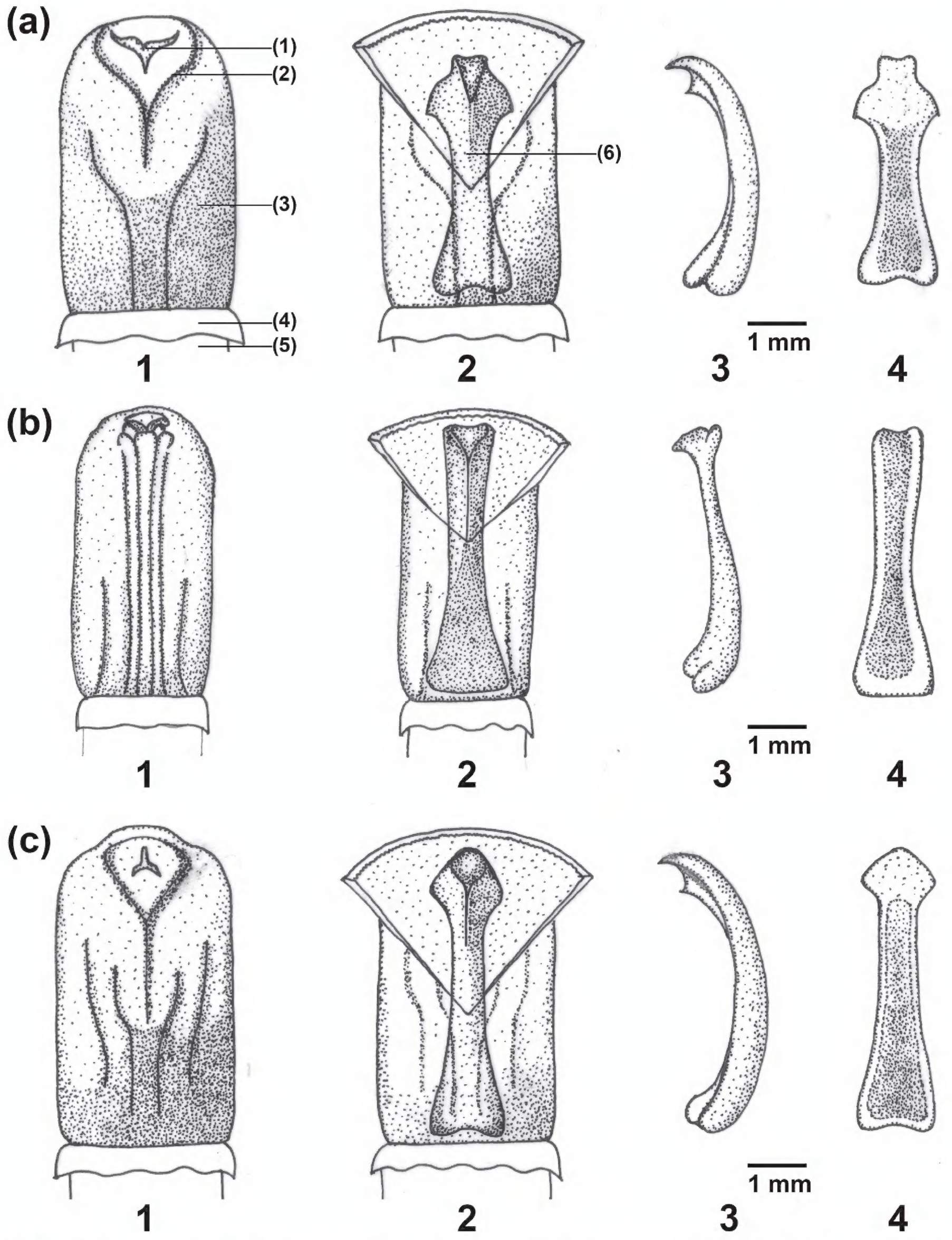

Figure 5. Comparison of the glans penis of three species within the *S. concolor* group. **a.** *Sicista concolor*; **b.** *Sicista* sp2; **c.** *Sicista weigoldi*. 1. Penis; 2. Midventral cut view of glans; 3. Lateral view of baculum; 4. Dorsal view of baculum. (1) Urethral opening; (2) Outer crater; (3) Glans; (4) Prepuce; (5) Body of penis; (6) Baculum.

during the Late Miocene to Late Pliocene (11.6–2.58 Ma), particularly affecting the Hengduan Mountains and adjacent regions (Clark et al. 2005; Wang et al. 2012). We hypothesize that the divergence between *S. tianschanica* and its sister clades (8.96 Ma) may represent an early evolutionary response to the initial phases of this uplift. In contrast, the subsequent diversification within the *S. concolor* group (5.87–2.96 Ma) likely reflects the continued topographic reorganization and climatic oscillations during the Late Neogene.

The origin of the *Sicista* has been a long-standing topic of debate, and our study may provide new insights into this issue. Previous molecular evidence suggested that *S. tianschanica* is positioned at the base of the phylogenetic tree, followed by *S. concolor* (Zhang et al. 2013, Pisano et al. 2015), implying that *S. tianschanica* might be the sister species to other *Sicista* species. Cserkész et al. (2017) noted that the penile structure of *S. concolor* is relatively simple compared to *S. tianschanica* and *S. caudata*, suggesting that *S. concolor* might represent a more ancient morphological form. The phylogenetic tree shows that *S. concolor* is not the earliest diverging species; therefore, it is hypothesized to be a basal species within the genus. They also emphasized the need for additional samples from other species, such as *S. caudata* and *S. leathemi*, to further test this hypothesis (Cserkész et al. 2017). Lebedev et al. (2019) divided the *Sicista* genus into five major clades: "*tianschanica*," "*concolor*," "*caudata*," "*betulina*," and "*caucasica*." The latter three clades received strong support, but the "*tianschanica*" clade, as the sister group to other species, had relatively low support, possibly due to limited genetic data from *S. concolor*. Lebedev et al. (2019) also pointed out that due to the scarcity of data for *S. concolor* and the absence of *S. leathemi* samples, the hypothesis of *S. concolor*'s origin remains unconfirmed. In our study, we included many of the *S. concolor* group specimens and constructed a phylogenetic tree based on nuclear genes. Our results show that *S. tianschanica* occupies the most basal position within the genus, followed by *S. concolor* (Fig. 3). According to Cserkész et al. (2017), *S. tianschanica* displays keratinized spines on the lateral view of the glans, whereas *S. concolor* lacks such spines in the dorsal view. However, based on our observations, all three members of the *S. concolor* group examined in this study possess distinct keratinized spines. This discrepancy may be attributed to geographic variation in sampling locations and warrants further investigation with broader geographic sampling. From a morphological perspective, the glans structures of *S. tianschanica* and the *S. concolor* group members suggest that these taxa are unlikely to represent the most basal lineages within the genus. This result is largely consistent with previous studies, suggesting that *S. concolor* may not be the oldest species in the genus. Notably, we discovered a clade (GenBank: PQ227707) at the base of the mitochondrial gene tree from a specimen collected in Tibet (Himalayan region), strongly supported (PP > 0.9, BS > 70). This clade shows distinct morphological differences from the other *Sicista* species, such as the absence of the incisor foramina crossing the anterior edge of the first upper molar or even failing to reach the anterior edge of the premolar. Molecular differences also support the distinction (Fig. 2a). Additionally, existing fossil evidence suggests that the *Sicista* genus may have originated in Central Asia (Lebedev et al. 2019). Therefore, we hypothesize that there may be some unstudied, ancient *Sicista* populations in the Himalayan region. Given their more ancient position, this may help explain the relatively low support for *S. concolor* in the phylogenetic tree (Cserkész et al. 2017) and the weak branch support in the phylogeny of the *Sicista* (Lebedev et al. 2019). In conclusion, the origin of the *Sicista* group remains unresolved, and further sampling and comparison of different regional clades are needed to provide a clearer answer to this issue.

Taxonomic account

Family Sicistidae Allen, 1901
Genus *Sicista* Gray, 1827

***Sicista meiguites* Deng Y, Liu Q, Wang XM, Liu SY & Chen SD, sp. nov.**

https://zoobank.org/69B96419-F155-402B-9673-333A424001FE

Holotype. SAF191012, an adult female collected from Dafengding Nature Reserve in June 2019 by Binbin V. Li. The specimen, preserved as dry skin, skull, and muscle and liver tissues in 95% ethanol, was deposited at the Sichuan Academy of Forestry. The external and cranial measurements (in millimeters) are as follows: HBL = 64 mm, TL = 117 mm, HFL = 19 mm, EL = 13 mm, PL = 20.96 mm, SBL = 16.33 mm, MPL = 9.95 mm, LBO=4.14mm,BB=9.30mm,HB=7.46mm,ABL=5.63mm, UTRL = 9.22 mm, LUM = 3.00 mm, UMRB = 4.10 mm, ML = 12.66 mm, LTRL = 8.29 mm, and LLMR = 3.05 mm.

Type locality. Dafengding National Nature Reserve, Meigu County, Liangshan Yi Autonomous Prefecture, Sichuan Province, China (28.6116°N, 102.9418°E, 2939 m).

Paratype. SAF06183, SAF06149, adult male captured (28.72102°N, 103.27753°E, 2500 m) in June 2006 by SY Liu, Y Liu, YD Li, and J Zhao. SAF07057, SAF07058, adult male captured on May 12, 2007, by Y Liu and QX Xiao. SAF191015, SAF191178, SAF191056, SAF191014, SAF191056 collected from Dafengding National Nature Reserve in 2019 by Binbin V. Li. All specimens are deposited at the Sichuan Academy of Forestry.

Diagnosis. This species is distinguished by its unique tail (Fig. 7b1–b3). The tail is darker than that of other species, displaying a deep brown color with a tuft of black hairs at the tip, and its length is approximately twice the length of the body. The palatine foramina are aligned along a line connecting the protocone and paracone of the second upper molar, and the distance between them exceeds the transverse width of the incisive foramen (Fig. 6b5).

Description. The head and body length ranges from 53 to 70 mm, tail length from 86 to 145 mm, hind foot length from 16 to 21 mm, ear length from 10 to 17 mm, head length from 18 to 22 mm, and body weight from 6 to 14 g. The upper lip is divided into two segments. The cheeks are tea yellow, extending from the back of the neck to beneath the ears and to the front of the shoulders. Each side has more than 20 vibrissae, with the longest whiskers reaching approximately 30 mm. The longer whiskers are black in the middle and lower parts, grayish-white in the middle and upper parts, while the shorter whiskers are almost entirely grayish-white. The ears are small and

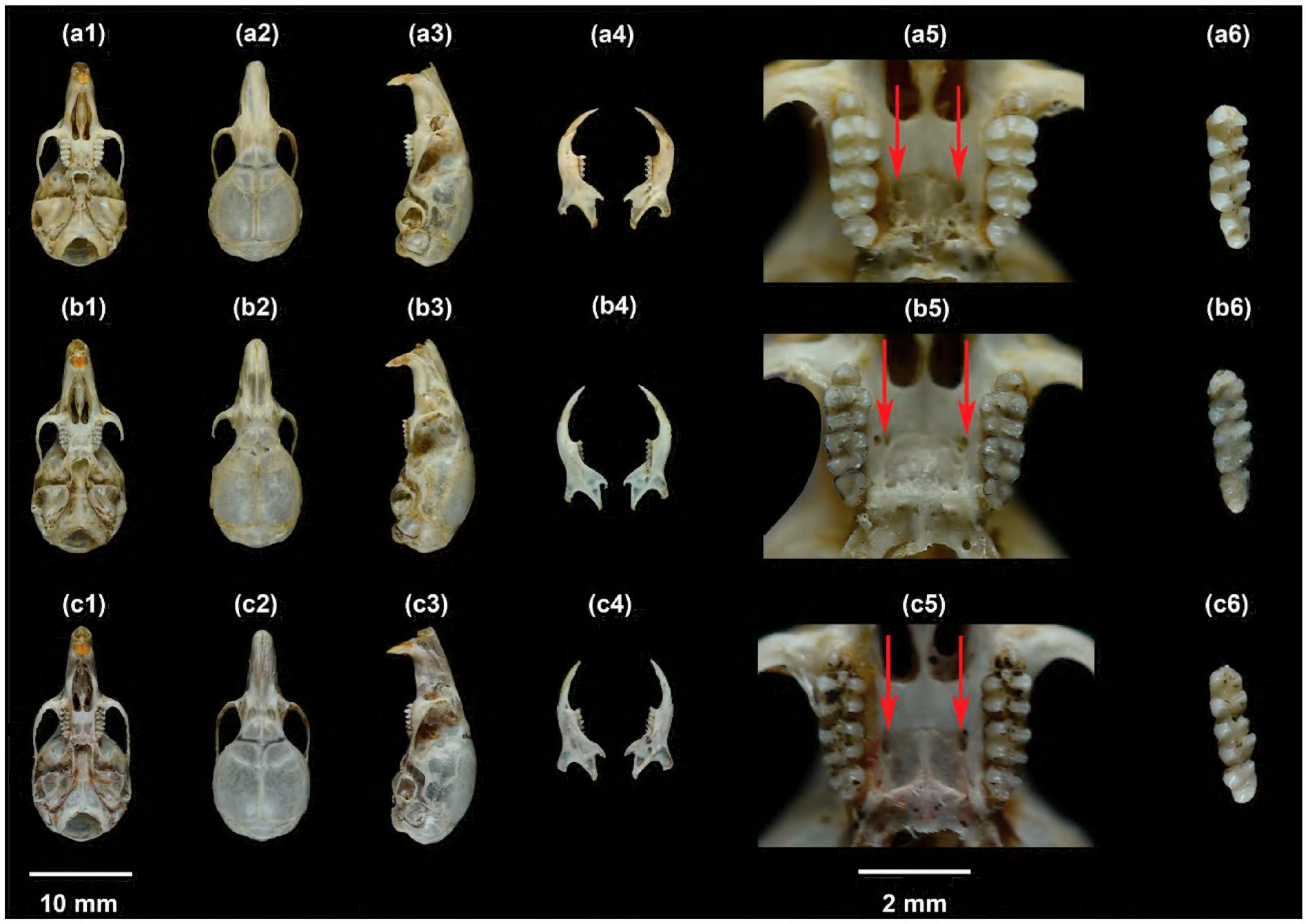

Figure 6. Skulls and tooth comparison among species of the *S. concolor* group. **a.** *Sicista concolor* (**a1–a6**) (museum number: SAF13331); **b.** *Sicista meiguites* sp. nov. (**b1–b6**) (museum number: SAF191012); **c.** *Sicista weigoldi* (**c1–c6**) (museum number: SAF240595).

Figure 7. Pelage and tail comparisons among species of the *S. concolor* group. **a.** *Sicista concolor* (**a1–a3**) (museum number: SAF13331); **b.** *Sicista meiguites* sp. nov. (**b1–b3**) (museum number: SAF191014); **c.** *Sicista weigoldi* (**c1–c3**) (museum number: SAF240595).

round, covered with dark brown short fur. The dorsal fur is dark brown, without any black stripes. The ventral fur has a light gray base with pale yellow tips, and there is no clear demarcation between the back and belly fur. The tail is dark brown and uniformly colored, about twice the length of the head and body. The feet are dark brown, with white toes, and there are long white hair tufts at the base of the claws. The hind limbs are relatively short, with the hind foot length smaller than the total skull length, making them unsuitable for jumping. The forelimbs have four toes, and the hind limbs have five toes (Fig. 7b1–b3).

The cranial region is roughly oval in shape, characterized by a relatively short rostrum. The anterior end of the nasal bone slightly extends beyond the maxillary premaxilla and upper incisors. There is no prominent supraorbital ridge between the orbits. The interorbital region is relatively broad, with the narrowest point located at the midline of the frontal bone. The width of the interparietal bone is about twice its length. The posterior margin of the palatine bone is slightly protruding, extending beyond the posterior margin of the molars. The palatine foramen of the upper jaw are located along the line connecting the protocone and paracone of the second upper molar. The distance between the paired palatine foramina exceeds the width between the lateral margins of the incisive foramen. The coronoid process, condyloid process, and angular process of the mandible are all pointed and slant posteriorly, with thin bones connecting the central region (Fig. 6b1–b5).

The length of the upper dental row ranges from 9.17 to 9.28 mm, and the length of the lower dental row ranges from 8.08 to 8.32 mm. The upper incisors are slender, oriented vertically toward the ventral side, with an orange enamel surface on the labial side, lacking vertical grooves. The lower incisors are white. The width of the upper molar row is 4.10–4.34 mm, and the length is 3.00–3.12 mm. The upper premolar is very small and cylindrical in shape. The first and second upper molars are well-developed, each bearing four cusps with deep folds on both the inner and outer sides. The anterior margin of the first molar forms a small protuberance that is lower than the cusps. The second molar is equal in size to the first molar. The third upper molar is very small, circular, and shows signs of gradual degeneration. The lower molar row measures 2.90–3.12 mm in length. The mandible contains three molars. The first lower molar aligns with the second upper molar. Both the first and second lower molars are quadrangular, with four distinct cusps and well-developed central depressions. The anterior margin of the first lower molar features a protuberance. The third lower molar is larger than the third upper molar and exhibits a notch along its inner edge (Fig. 6b5–b6).

The glans penis is relatively slender and covered with distinct, evenly distributed keratinized spines. There are 1–2 longitudinal grooves running along the ventral midline and a single longitudinal groove on the dorsal side. The urethral opening is Y-shaped. The outer annular layer lacks papillae, and no urethral valves, dorsal projections, or lateral branches are observed. The baculum exhibits an ossified, rod-like structure without differentiation into distal and proximal ends. The base is slightly concave, and the overall shape is markedly curved towards the ventral side. The ventral tip is Y-shaped, with a central longitudinal groove, and an additional groove is present on the dorsal side (Fig. 5b1–b4).

Comparisons. Compared to *S. concolor*, it has a deep, uniformly colored tail measuring over 180% of the head-body length. The base of the limbs is covered with dark brown fur (Fig. 7). In particular, the palatine foramen of the upper jaw is located along the line connecting the original and anterior cusps of the second upper molar, and the distance between the palatine foramen and the incisor foramen margin exceeds the width of the incisor foramen itself (Fig. 6). Additionally, the tooth row of *S. concolor* forms a pronounced arc, with the last pair of molars markedly inclined inward (Fig. 6a5), whereas *S. weigoldi* has a straight tooth row (Fig. 6c5). The new species exhibits an intermediate dental configuration between these two conditions (Fig. 6b5).

Etymology. This newly discovered species was found in Meigu, Sichuan Province. In recognition of its type locality, we have named the species accordingly. We propose the English name "Meigu Birch Mouse" and the Chinese name "美姑蹶鼠" for this species.

Distribution. It is currently known only from Meigu, Sichuan Province, and inhabits the shaded tall grass in montane and subalpine coniferous forests, mixed conifer-broadleaf forests, riverside shrublands, meadows, and alpine grasslands at altitudes ranging from 2000 to 3000 meters.

Sicista concolor (Büchner, 1892)

Type locality. Xining City, Qinghai Province, China.

Diagnosis. The brown tail is unicolored and measures approximately 150–170% of the head-body length. The back of the body is brown, lacking black stripes along the spine, and the abdomen is light brown in color (Fig. 7a1–a3). The Palatine Foramina are located along the line connecting the metacone and the hypocone of the second upper molar (Fig. 6a5).

Remarks. A small jerboa, with a body length ranging from 65 to 73 mm, tail length from 103 to 122 mm, hind foot length from 18 to 20 mm, ear length from 12 to 16 mm, and body weight between 10 and 13 g (Table 2). The dorsal fur is brown, interspersed with black hairs, and lacks distinct vertical black stripes along the spine (Fig. 7a1–a3). The glans penis is relatively short and thick, with a surface densely covered in evenly distributed keratinized spines. The urethral opening is elongated and Y-shaped, while the external tissue surrounding the urethral opening forms a U-shape. The outer annular layer lacks papillae, and no urethral valves, dorsal projections, or lateral branches are observed. The baculum exhibits an ossified, rod-like structure with two lateral wings at the tip. The base is slightly concave, without differentiation into distal and proximal ends. It has a tendency to curve ventrally. The ventral tip is Y-shaped, with a central longitudinal groove, and an additional groove is present on the dorsal side (Fig. 5a1–a4).

This species is extremely rare in the wild. Specimens are only available from Qinghai Province, and there is limited knowledge regarding populations in Gansu and

Table 2. Measurement data of skull morphological indexes of the *S. concolor* group (in millimeters).

Measurement	*S. concolor*	*S.* sp2	*S. weigoldi*
	n = 4	n = 4	n = 21
HL	70.00 ± 3.46	63.75 ± 2.36	63.19 ± 6.68
	65–73	62–67	50–75
TL	114.67 ± 10.21	130.75 ± 9.54	119.86 ± 13.27
	103–122	117–139	86–138
HFL	16.50 ± 5.07	19.50 ± 0.58	18.29 ± 1.27
	9–20	19–20	16–21
EL	14.75 ± 1.89	13.25 ± 0.50	13.76 ± 2.02
	12–16	13–14	10–16
PL	20.68 ± 0.55	20.96 ± 0.03	20.31 ± 1.00
	20.09–21.17	20.93–21.00	18.17–21.67
SBL	16.24 ± 0.38	16.33 ± 0.05	16.48 ± 1.12
	15.90–16.71	16.26–16.37	13.81–17.82
MPL	10.18 ± 0.37	9.95 ± 0.09	10.04 ± 0.76
	9.87–10.65	9.83–10.03	8.46–11.29
LBO	4.13 ± 0.09	4.16 ± 0.02	4.03 ± 0.17
	4.07–4.26	4.14–4.19	3.58–4.41
BB	9.67 ± 0.24	9.32 ± 0.09	9.39 ± 0.40
	9.41–9.88	9.22–9.43	8.47–9.92
BH	7.41 ± 0.22	7.46 ± 0.03	7.41 ± 0.34
	7.13–7.64	7.44–7.50	6.53–7.91
ABL	6.28 ± 0.65	5.67 ± 0.10	5.63 ± 0.21
	6.22–6.37	5.55–5.75	4.85–5.87
UTRL	9.36 ± 0.12	9.22 ± 0.05	9.17 ± 0.41
	9.23–9.51	9.17–9.28	8.33–9.84
LUM	3.25 ± 0.09	3.05 ± 0.05	3.10 ± 0.18
	3.15–3.34	3.00–3.12	2.80–3.47
UMR	4.33 ± 0.10	4.26 ± 0.11	4.29 ± 0.20
	4.25–4.47	4.10–4.34	3.94–4.64
ML	12.30 ± 0.12	12.50 ± 0.14	12.28 ± 0.61
	12.17–12.44	12.37–12.66	11.08–13.16
LTRL	8.22 ± 0.01	8.24 ± 0.11	8.07 ± 0.29
	8.09–8.32	8.08–8.32	7.60–8.71
LLMR	3.17 ± 0.01	3.02 ± 0.09	3.06 ± 0.20
	3.15–3.18	2.90–3.12	2.73–3.47

Table 3. Percent variance explained on the two components of PCA of cranial measurements of the *S. concolor* group.

Variables	PC1	PC2
UTRL	0.925	0.006
SBL	0.919	-0.141
MPL	0.887	-0.149
UMRB	0.885	0.250
LTRL	0.875	-0.246
BB	0.870	-0.044
LLMR	0.835	-0.424
ML	0.824	0.146
PL	0.797	0.373
HB	0.741	0.054
LUM	0.703	-0.513
LBO	0.629	0.412
ABL	0.379	0.756
Eigenvalues	8.383	1.516
Variance explained (%)	64.484	11.661

Shaanxi Provinces. The geographical isolation caused by numerous mountain ranges and rivers may have led to the formation of distinct species. Further sampling is necessary to verify this hypothesis.

Distribution. This species is distributed along the northeastern edge of the Tibetan Plateau, primarily in the provinces of Gansu, Qinghai, and Shaanxi, China. It is commonly found in temperate forest edges, shrublands, and grassland shrub communities. The species constructs nearly spherical nests made of grass, typically placed in the gaps between shrubs.

Sicista weigoldi Jacobi, 1923

Type locality. Songpan County, Sichuan Province, China.

Diagnosis. The tail exhibits a distinct bicolored pattern, with the dorsal surface being brown and the ventral surface slightly lighter, devoid of a tuft of hair at the tip (Fig. 7c1–c3). The palatine foramen in the upper jaw is positioned along the midline of the second upper molar, with the distance between the two foramina not exceeding the width of the incisor foramen (Fig. 6c1–c5).

Remarks. The glans penis is relatively short and thick, covered with keratinized spines. The urethral opening is not Y-shaped, and the external tissue surrounding the urethral opening forms a U-shape. A shallow groove is present at the base of the dorsal midline, but no lateral grooves are observed. The outer annular layer lacks papillae, and no urethral valves, dorsal projections, or lateral branches are present. The baculum exhibits an ossified, rod-like structure. In most individuals, the tip possesses two lateral wings, resembling a "cobra hood," while in a few individuals, it remains a slender rod, possibly due to incomplete ossification of the cartilage. There is no differentiation between distal and proximal ends, and it tends to curve ventrally. The ventral tip is Y-shaped, with a central longitudinal groove, and an additional groove is present on the dorsal side (Fig. 5c1–c4).

S. weigoldi (Jacobi 1923) was first discovered in Songpan and is characterized by a distinct bicolored tail, with the dorsal side brown and the ventral side white. It was initially considered a junior synonym of *S. concolor* (Allen 1940). Subsequently, *S. weigoldi* was often regarded as a subspecies of *S. concolor* (Wilson and Reeder 1993; Csekész et al. 2017). However, Lebedev et al. (2019) proposed that it may represent a distinct species due to significant geographic isolation. Based on both molecular and morphological evidence, our results support this hypothesis, thereby elevating it to a valid species.

Distribution. This species is distributed in areas such as Songpan, Pingwu, and Jiuzhaigou in Sichuan Province, inhabiting moist montane coniferous forests, birch forests, and alpine meadows at elevations between 2000 and 4000 meters.

Sicista leathemi Thomas, 1893

Type locality. the Kashmir region.

Diagnosis. Compared to other birch mice, the incisor foramina is shorter, extending posteriorly only to the middle level of the first molar, with the posterior end of the maxilla near the anterior edge of the molars.

Remarks. The tail is brown with a bicolored pattern. The dorsal body is brown, with no dark stripes along the midline, while the ventral fur is grayish-white, with an

Table 4. Morphology comparison of the *S. concolor* group.

Species	*S. concolor*	*Sicista meiguites* sp. nov.	*S. weigoldi*
Tail	Brown hairs with a monochromatic appearance. The tail length is approximately 50% to 70% longer than the head-body length.	Dark brown hairs with a monochromatic appearance. The tail length exceeds the head-body length by more than 80%.	Brown with a heterochromatic pattern. The tail length is approximately twice the head-body length.
Limbs	Forefoot with short white hairs on the dorsum and base.	The base of the limbs is covered with dark brown hair.	Forefoot is back with short white hair.
Palatine foramina	Located on the metacone and the hypocone line of the second upper molar.	Located along the line connecting the paracone and protocone of the second upper molar.	Located on the central line of the second upper molar;
	The distance between the two palatine foramen is smaller than the distance to the edge of the incisor foramen.	The distance between the palatine foramen is significantly greater than the width of the incisor.	The distance between the two palatine foramen is less than the edge of the incisor.
The glans penis	Relatively short and thick, with a Y-shaped urethral opening. The baculum tip generally exhibits two lateral wings.	Relatively slender, with a Y-shaped urethral opening. The baculum is ossified and rod-shaped.	Relatively short and thick, with a non-Y-shaped urethral opening. The baculum tip generally exhibits two lateral wings.

indistinct boundary between the dorsal and ventral regions. The tips of the fur are russet, interspersed with longer, coarser black hairs, with the base of the fur grayish-white. The claws are long and prominent, with a dull grayish-white surface. The hindfoot is entirely white, with no plantar pads, while the back of the front feet is dark brown, and the toes are white.

S. leathemi is typically considered a subspecies of *S. concolor*. However, Lebedev et al. (2019) proposed that it might represent a distinct species. Liu et al. (2025) proposed restoring *S. leathemi* to species status based on mitochondrial gene data and morphological evidence. Our findings also support this possibility (Fig. 2a).

Distribution. It is distributed in the alpine or subalpine scrub regions of the Himalayas, with reports from areas such as Kashmir and Tibet, China.

Conclusion

This study explores the phylogenetic relationships and evolutionary history of the *Sicista concolor* group using molecular and morphological data, particularly emphasizing the importance of the morphology of the penis. Both molecular and morphological results support the division of this group into three valid, independent species: *S. concolor*, *S. weigoldi*, and *S. meiguites* sp. nov. *S.* sp1 is currently designated as a cryptic species. Additionally, our divergence time tree suggests that the diversification of the *S. concolor* group may be linked to Pleistocene climate changes and the uplift of the Tibetan Plateau. Finally, a review of the *S. concolor* group taxa is provided, along with features for identification.

Acknowledgements

This work was supported by the National Natural Science Foundation of China (32370496) to Liu Shaoying, the Survey of Wildlife and Plant Resources in Key Regions of Tibet (ZL202203601) to Liu Shaoying, the National Natural Science Foundation of China (32070424) to Chen Shunde, and the Natural Science Foundation of Sichuan Province (2025ZNSFSC0277) to Chen Shunde.

References

Allen GM (1940) The mammals of China and Mongolia. American Museum of Natural History, 11, part 2: 621–1350.

Baskevich MI (2016) Taxonomy, evolution and variation of the genus *Sicista* (Rodentia, Dipodoidea): A review of karyological and molecular data. Archives of Zoological Museum of Lomonosov Moscow State University 54: 191–228. [In Russian]

Büchner E (1892) Über eine neue *Sminthus*-Art aus China. Bulletin de l'Académie impériale des sciences de St.-Pétersbourg 35(3): 107–109.

Chen ZZ, He K, Huang C, Wan T, Lin LK, Liu SY, Jiang XL (2017) Integrative systematic analyses of the genus *Chodsigoa* (Mammalia: Eulipotyphla: Soricidae), with descriptions of new species. Zoological Journal of the Linnean Society 180(3): 694–713. https://doi.org/10.1093/zoolinnean/zlw017

Cheng JL, Xia L, Wen ZX, Zhang Q, Ge DY, Yang QS (2021) Review on the systematic taxonomy of *Dipodoidea* in China. Acta Theriologica Sinica 41(3): 275–283.

Clark MK, House MA, Royden LH, Whipple KX, Burchfiel BC, Zhang X, Tang W (2005) Late Cenozoic uplift of southeastern Tibet. Geology 33(6): 525. https://doi.org/10.1130/G21265.1

Corbet GB (1978) *The mammals of the Palaearctic region: A taxonomic review*. British Museum (Natural History) and Cornell University Press.

Cserkész T, Fülöp A, Almerekova S, Kondor T, Laczkó L, Sramkó G (2017) Phylogenetic and morphological analysis of birch mice (genus *Sicista*, family Sminthidae, Rodentia) in the Kazak cradle with description of a new species. Journal of Mammalian Evolution 26(1): 147–163. https://doi.org/10.1007/s10914-017-9409-6

Darriba D, Taboada GL, Doallo R, Posada D (2012) jModelTest 2: More models, new heuristics and parallel computing. Nature Methods 9(8): 772. https://doi.org/10.1038/nmeth.2109

Drummond AJ, Suchard MA, Xie D, Rambaut A (2012) Bayesian phylogenetics with BEAUti and the BEAST 1.7. Molecular Biology and Evolution 29(8): 1969–1973. https://doi.org/10.1093/molbev/mss075

Ellerman JR, Morrison-Scott TCS (1951) Checklist of Palaearctic and Indian mammals 1758 to 1946. British Museum (Natural History).

He K, Shinohara A, Helgen KM, Springer MS, Jiang X-L, Campbell KL (2017) Talpid mole phylogeny unites shrew moles and illuminates overlooked cryptic species diversity. Molecular Biology and Evolution 34(1): 78–87. https://doi.org/10.1093/molbev/msw221

Ho SY (2007) Calibrating molecular estimates of substitution rates and divergence times in birds. Journal of Avian Biology 38(4): 409–414. https://doi.org/10.1111/j.0908-8857.2007.04168.x

Holden ME, Musser GG (2005) Superfamily Dipodoidea. In: Wilson DE, Reeder DM (Eds) Mammal species of the world (3rd edn.). Johns Hopkins University Press, 871–893.

Holden ME, Cserkész T, Musser GG (2017) Family Sminthidae. In: Wilson DE, Lacher TE, Mittermeier RA (Eds) Handbook of the mammals of the world, Vol. 7: Rodents II. Lynx Ediciones, 22–48.

Hooper ET (1958) The male phallus in mice of the genus *Peromyscus*. Miscellaneous Publications (University of Michigan. Museum of Zoology) 623: 1–18. https://doi.org/10.3998/mpub.12946894

Howell AB (1929) Mammals from China in the collections of the United States National Museum. Proceedings of the United States National Museum 75(1): 1–82. https://doi.org/10.5479/si.00963801.75-2772.1

Jacobi A (1923) Zoologische Ergebnisse der Walter Stötznerschen Expeditionen nach Szetschwan, Osttibet und Tschili auf Gr- und der Sammlungen und Beobachtungen Dr. Hugo Weigolds. Abhandlungen und Berichte der Museen für Tierkunde und Völkerkunde zu Dresden 16(1): 15.

Jiang Z, Ma Y, Wu Y, Wang Y, Feng Z, Zhou K, Liu S, Luo Z, Li C (2015) China's mammalian diversity. Biodiversity Science 23(3): 351. https://doi.org/10.17520/biods.2014202

Kimura M (1980) A simple method for estimating evolutionary rates of base substitutions through comparative studies of nucleotide sequences. Journal of Molecular Evolution 16(2): 111–120. https://doi.org/10.1007/BF01731581

Kowalski K (2001) Pleistocene rodents of Europe. Folia Quaternaria 72: 1–382.

Lebedev VS, Bannikova AA, Pagès M, Pisano J, Michaux JR, Shenbrot GI (2013) Molecular phylogeny and systematics of Dipodoidea: A test of morphology-based hypotheses. Zoologica Scripta 42(3): 231–249. https://doi.org/10.1111/zsc.12002

Lebedev VS, Rusin MY, Zemlemerova ED, Matrosova VA, Bannikova AA, Kovalskaya YM, Tesakov AS (2019) Phylogeny and evolutionary history of birch mice *Sicista* Griffith, 1827 (Sminthidae, Rodentia): Implications from a multigene study. Journal of Zoological Systematics and Evolutionary Research 57(4): jzs.12279. https://doi.org/10.1111/jzs.12279

Lidicker WZ (1968) A phylogeny of New Guinea rodent genera based on phallic morphology. Journal of Mammalogy 49: 609–643. https://doi.org/10.2307/1378724

Liu SY, Sun ZY, Zeng ZY, Zhao EM (2007) A new species (*Proedomys*: Arvicolinae: Muridae) from the Liangshan Mountains of Sichuan Province, China. Journal of Mammalogy 5: 1170–1178. https://doi.org/10.1644/06-MAMM-A-141R2.1

Liu SY, Liu Y, Guo P, Sun ZY, Murphy RW, Fan ZX, Fu JR, Zhang YP (2012) Phylogeny of oriental voles (Rodentia: Muridae: Arvicolinae): Molecular and morphological evidence. Zoological Science 29(9): 610–622. https://doi.org/10.2108/zsj.29.610

Liu SY, Jin W, Liao R, Sun ZY, Zeng T, Fu JR, Liu Y, Wang X, Li PF, Tang MK, Chen LM, Dong L, Han MD, Gou D (2017) Phylogenetic study of *Ochotona* based on mitochondrial *Cyt b* and morphology with a description of one new subgenus and five new species. Acta Theriologica Sinica 37(1): 1–43. https://doi.org/10.16829/j.slxb.201701001

Liu SY, Chen SD, He K, Tang M, Liu Y, Jin W, Li S, Li Q, Zeng T, Sun ZY, Fu JR, Liao R, Meng Y, Wang X, Jiang XL, Murphy RW (2019) Molecular phylogeny and taxonomy of subgenus *Eothenomys* (Cricetidae: Arvicolinae: *Eothenomys*) with the description of four new species from Sichuan, China. Zoological Journal of the Linnean Society 186(2): 569–598. https://doi.org/10.1093/zoolinnean/zly071

Liu YX, Peng BQ, Wang XM, Liao R, Pan X, Liu SY (2025) The list of the mammals in Xizang added a new family-Sicistidae. Acta Theriologica Sinica. https://doi.org/10.16829/j.slxb.151005

Lu HQ, Li YC, Zhang XD (1987) Age determination, age structure and population dynamics of striped hamster. Acta Theriologica Sinica 7(1): 35–45.

Luo A, Qiao H, Zhang Y, Shi W, Ho SY, Xu W, Zhang A, Zhu C (2010) Performance of criteria for selecting evolutionary models in phylogenetics: A comprehensive study based on simulated datasets. BMC Evolutionary Biology 10(1): 242. https://doi.org/10.1186/1471-2148-10-242

Meredith RW, Janečka JE, Gatesy J, Ryder OA, Fisher CA, Teeling EC, Goodbla A, Eizirik E, Simão TLL, Stadler T, Rabosky DL, Honeycutt RL, Flynn JJ, Ingram CM, Steiner C, Williams TL, Robinson TJ, Burk-Herrick A, Westerman M, Ayoub NA, Springer MS, Murphy WJ (2011) Impacts of the Cretaceous terrestrial revolution and KPg extinction on mammal diversification. Science 334(6055): 521–524. https://doi.org/10.1126/science.1211028

Miller MA, Pfeiffer W, Schwartz T (2010) Creating the CIPRES science gateway for inference of large phylogenetic trees. 2010 Gateway Computing Environments Workshop (GCE), 1–8. https://doi.org/10.1109/GCE.2010.5676129

Pallas PS (1773) Reise durch verschiedene Provinzen des Russischen Reichs 1(2). Kaiserliche Academie der Wissenschaften, 705–706.

Paradis E, Claude J, Strimmer K (2004) APE: Analyses of phylogenetics and evolution in R language. Bioinformatics 20(2): 289–290. https://doi.org/10.1093/bioinformatics/btg412

Pisano J, Condamine FL, Lebedev V, Bannikova A, Quéré J, Shenbrot GI, Pagès M, Michaux JR (2015) Out of Himalaya: The impact of past Asian environmental changes on the evolutionary and biogeographical history of Dipodoidea (Rodentia). Journal of Biogeography 42(5): 856–870. https://doi.org/10.1111/jbi.12476

Pons J, Barraclough TG, Gomez-Zurita J, Cardoso A, Duran DP, Hazell S, Kamoun S, Sumlin WD, Vogler AP (2006) Sequence-based species delimitation for the DNA taxonomy of undescribed insects. Systematic Biology 55(4): 595–609. https://doi.org/10.1080/10635150600852011

Pu YT, Wan T, Fan RH, Fu CK, Tang KY, Jiang XL, Zhang BW, Hu TL, Chen SD, Liu SY (2022) A new species of the genus *Typhlomys* Milne-Edwards, 1877 (Rodentia: Platacanthomyidae) from Chongqing, China. Zoological Research 43(3): 413–417. https://doi.org/10.24272/j.issn.2095-8137.2021.338

Rambaut A (2016) FigTree v.1.4.3. Retrieved from http://tree.bio.ed.ac.uk/software/figtree/

Rambaut A, Drummond A (2013) Tracer 1.6. University of Edinburgh. [Software documentation]

Salensky W (1903) Über eine neue *Sminthus*-Art aus dem Tianschan (*Sminthus tianschanicus* n. sp.; Rodentia Dipodiade). Yearbook of Zoological Museum of Academy of Sciences 8: 17–21.

Smith AT, Hoffmann RS, Lunde D, MacKinnon J, Wilson DE, Wozencraft WC, Gemma F, Sung W (2008) Taxonomic descriptions. In: Smith AT, Xie Y (Eds) A guide to the mammals of China. Princeton University Press, 155–484.

Stamatakis A, Hoover P, Rougemont J (2008) A rapid bootstrap algorithm for the RAxML web servers. Systematic Biology 57(5): 758–771. https://doi.org/10.1080/10635150802429642

Strautman EI (1949) A new species of birch mouse from Kazakhstan. Vestnik Akademii Nauk Kazakhskoĭ SSR 5(10): 109–110.

Tamura K, Peterson D, Peterson N, Stecher G, Nei M, Kumar S (2011) MEGA5: Molecular evolutionary genetics analysis using maximum

likelihood, evolutionary distance, and maximum parsimony methods. Molecular Biology and Evolution 28(10): 2731–2739. https://doi.org/10.1093/molbev/msr121

Thomas O (1893) Description of a new species of *Sminthus* from Kashmir. The Annals and Magazine of Natural History, Series 6 11(62): 184. https://doi.org/10.1080/00222939308677489

Thomas O (1907) The Duke of Bedford's zoological exploration in Eastern Asia. IV. List of small mammals from the Islands of Saghalien and Hokkaido. Proceedings of the General Meetings for Scientific Business of the Zoological Society of London 77(2): 404–414. https://doi.org/10.1111/j.1096-3642.1907.tb01825.x

Thomas O (1912) On a collection of small mammals from the Tsinling mountains, Central China, presented by Mr. G. Fenwick Owen to the National Museum. Annals & Magazine of Natural History 10(58): 401. https://doi.org/10.1080/00222931208693252

Wang E, Kirby E, Furlong KP, van Soest M, Xu G, Shi X, Kamp PJJ, Hodges KV (2012) Two-phase growth of high topography in eastern Tibet during the Cenozoic. Nature Geoscience 5(9): 640–645. https://doi.org/10.1038/ngeo1538

Wei FW, Yang QS, Wu Y, Jiang XL, Liu SY (2024) Taxonomy and Distribution of Mammals in China. Science Press.

Wilson DE, Reeder DM (1993) Mammal species of the world: A taxonomic and geographic reference (2nd edn.). Smithsonian Institution Press.

Wilson DE, Reeder DM (2005) Mammal species of the world: A taxonomic and geographic reference (3rd edn., Vol. 1). Johns Hopkins University Press, 1–743.

Wu S, Wu W, Zhang F, Ye J, Ni X, Sun J, Edwards SV, Meng J, Organ CL (2012) Molecular and paleontological evidence for a post-cretaceous origin of rodents. PLoS ONE 7(10): e46445. https://doi.org/10.1371/journal.pone.0046445

Yang Z (2015) The BPP program for species tree estimation and species delimitation. Current Zoology 61: 854–865. https://doi.org/10.1093/czoolo/61.5.854

Yang AF, Fang LX (1988) Phallic morphology of 13 species of the family Muridae from China with comments on its taxonomic significance. Acta Theriologica Sinica 4: 275–285.

Yang Z, Rannala B (2010) Bayesian species delimitation using multilocus sequence data. Proceedings of the National Academy of Sciences of the United States of America 107(20): 9264–9269. https://doi.org/10.1073/pnas.0913022107

Yang QS, Xia L, Ma Y, Feng ZJ, Quan GQ (2005) A guide to the measurement of mammal skull I: Basic measurement. Chinese Journal of Zoology 40(3): 50–56.

Yang SY, Xie F, Zhou CX, Zhang ZY, Wang XM, Liu SY, Chen SD (2025) Molecular phylogeny and taxonomy of the genus *Eozapus* (Mammalia, Rodentia, Zapodidae) with the description of a new species. Zoosystematics and Evolution 101(2): 597–608. https://doi.org/10.3897/zse.101.133734

Zhang Q, Xia L, Kimura Y, Shenbrot G, Zhang Z, Ge D, Yang Q (2013) Tracing the origin and diversification of Dipodoidea (Order: Rodentia): Evidence from fossil record and molecular phylogeny. Evolutionary Biology 40: 32–44. https://doi.org/10.1007/s11692-012-9167-6

Zhao SP, Wang XM, Li BV, Dou L, Liu YX, Yang SY, Fan RH, Jiang Y, Li Q, Liao R, Hu M, Jiang XL, Liu SY, Chen SD (2023) Molecular phylogeny and taxonomy of the genus *Vernaya* (Mammalia: Rodentia: Muridae) with the description of two new species. Ecology and Evolution 13: e10628. https://doi.org/10.1002/ece3.10628

Supplementary material 1

Information on the sequence of specimens and outgroups in this study

Authors: Yu Deng, Qing Liu, Xuming Wang, Binbin V. Li, Jing Wang, Shuang Liu, Rui Liao, Shaoying Liu, Shunde Chen

Data type: docx

Link: https://doi.org/10.3897/zse.101.155510.suppl1

Supplementary material 2

Results of GMYC-based species delimitation based on CYTB gene

Authors: Yu Deng, Qing Liu, Xuming Wang, Binbin V. Li, Jing Wang, Shuang Liu, Rui Liao, Shaoying Liu, Shunde Chen

Data type: png

Link: https://doi.org/10.3897/zse.101.155510.suppl2

Supplementary material 3

Posterior probabilities for the 3 putative species using different priors for model parameters

Authors: Yu Deng, Qing Liu, Xuming Wang, Binbin V. Li, Jing Wang, Shuang Liu, Rui Liao, Shaoying Liu, Shunde Chen

Data type: docx

Explanation note: Text.

Link: https://doi.org/10.3897/zse.101.155510.suppl3